Performance Characteristics of Controlled Separately Excited DC Motor.

C.U. Ogbuka, M.Eng.

Department of Electrical Engineering, University of Nigeria, Nsukka, Enugu State.

E-mail: ucogbuka@yahoo.com

ABSTRACT

The control strategies, transfer functions, and performance analysis of Open Loop Control, Closed Loop Speed Control, and Inner Current Loop Controlled Separately Excited DC Motor are presented both for steady state and dynamic responses. For the Closed Loop Speed Control, three controllers are used, namely: Proportional, Integral, and Proportional-Integral Controllers. In the case of the Inner Current Loop Control, Proportional and Proportional-Integral Controllers are used for analysis. The results obtained show that the Open Loop Control gives a sluggish response which is improved in the Closed Loop Speed Control. The fastest response is obtained in the Inner Current Loop Control and this fast response and ease of control gives the DC Motor a competitive edge over the AC Motors. The analysis is presented in MATLAB/SIMULINK®.

(Keywords: DC motor, PID controller, speed control, MATLAB/SIMULINK)

INTRODUCTION

The applications of direct current (DC) machines have remained vital in industrial processes notwithstanding some competitive advantages of alternating current (AC) machines [1]. DC Motors have been widely used in many industrial applications such as electric vehicles, steel rolling mills, electric cranes, and robotic manipulators due to precise, wide, simple, and continuous control characteristics. Small DC motors (in fractional power rating) are used in control devices such as tacho-generators for speed sensing and servomotors for positioning and tracking [2].

Traditionally, the rheostatic armature control method was widely used for the speed control of low power DC motors. However the controllability, cheapness, higher efficiency, and higher current carrying capabilities of static power converters brought a major change in the performance of electrical drives [3].

The increasing complexity of industrial processes demands greater flexibility from electrical machines in terms of special characteristics and speed control [4]. Their torque/speed characteristics can be varied over a wide range, while the machine maintains its efficiency without sacrificing its speed as in the case of induction motors [5].

The controller configurations employed for this analysis, require exact mathematical modeling, the performance of the system for the three control configurations namely: Open Loop Control, Closed Loop Speed Control, and Inner Current Loop Control are carried-out and presented in MATLAB/SIMULINK® for performance comparison.

OPEN LOOP CONTROL

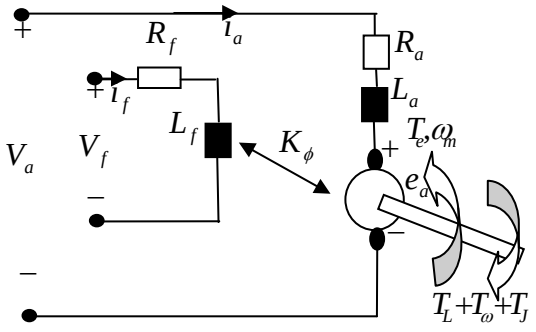

Figure 1: Schematic Diagram of Open Loop Control.

$$V_a = i_a R_a + e_a + L\frac{di_a}{dt} \qquad \textbf{(1)}$$

Taking the Laplace Transform:

$$V_a(s) = i_a(s)R_a + e_a(s) + sL_a i_a(s) \quad \textbf{(2)}$$

It, therefore, follows that

$$i_a = \frac{V_a - e_a}{R_a + sL_a} \quad \textbf{(3)}$$

It can be shown that the motor developed torque T_e is related to the armature current i_a as,

$$T_e = K_\phi i_a \quad \textbf{(4)}$$

And the armature induced emf is related to the motor speed as,

$$e_a = K_\phi \omega_m \quad \textbf{(5)}$$

Where K_ϕ is the field excitation constant.

Making reference to Figure 1,

$$T_e = T_\omega + T_J + T_L \quad \textbf{(6)}$$

Where $T_\omega = B\omega_m$ is the torque due to wind friction, B is the viscous frictional constant, and ω_m is the motor speed in rad/sec. $T_J = J\frac{d\omega_m}{dt}$ is the torque due to inertia of load and J is the motor and load inertia. Equation 6 modifies as

$$T_e = J\frac{d\omega_m}{dt} + B\omega_m + T_L \quad \textbf{(7)}$$

Taking the Laplace transform,

$$T_e = sJ\omega_m + B\omega_m + T_L \quad \textbf{(8)}$$

It is therefore realized that,

$$\omega_m = \frac{T_e - T_L}{Js + B} \quad \textbf{(9)}$$

The block diagram representation of the open loop control arrangement using Equations 3, 4, 5, and 9 is shown below:

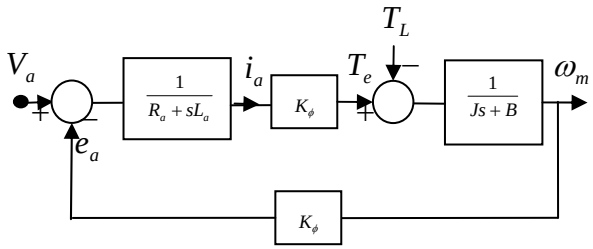

Figure 2: Block Diagram of the Open Loop Control.

Using Mason's rule, the dynamic equation is,

$$\begin{pmatrix} \omega_m \\ i_a \end{pmatrix} = \frac{\begin{pmatrix} K_\phi & -(R_a + sL_a) \\ Js + B & K_\phi \end{pmatrix}\begin{pmatrix} V_a \\ T_L \end{pmatrix}}{D_o(s)} \quad \textbf{(10)}$$

Where,

$$D_o(s) = s^2 JL_a + (R_a J + BL_a)s + R_a B + K_\phi^2 \quad \textbf{(11)}$$

This is a second order system with characteristic polynomial as,

$$D_o(s) = JL_a[s^2 + \frac{(R_a J + BL_a)}{JL_a}s + \frac{R_a B + K_\phi^2}{JL_a}] \quad \textbf{(12)}$$

$$D_o(s) = JL_a[s^2 + 2\varepsilon\omega_n s + \omega_n^2] \quad \textbf{(13)}$$

Where, ω_n is the Open Loop Drive Natural Frequency of Oscillation and ε the Open Loop Drive Damping Ratio. Comparing Equations 12 and 13, ω_n and ε are derived respectively as,

$$\omega_n = \sqrt{\frac{R_a B + K_\phi^2}{JL_a}} \quad \textbf{(14)}$$

$$\varepsilon = \frac{R_a + BL_a}{2\omega_n JL_a} \quad \textbf{(15)}$$

The Speed Regulation (SR) is derived as,

$$SR = \frac{-R_a}{R_a B + K_\phi^2} \quad \textbf{(16)}$$

Drive performance is measured as speed of response determined by ω_n, ε, and SR. The lower the Speed Regulation (SR), the faster the speed of response and the better the drive system [6].

The relationship between ω_n and T_L is,

$$\omega_m = \frac{K_\phi V_a - (R_a + sL_a)T_L}{D_o(s)} \quad \textbf{(17)}$$

At steady state, $s = 0$

$$\omega_m(\alpha) = \frac{K_\phi V_a - R_a T_L}{R_a B + K_\phi^2} \quad \textbf{(18)}$$

At constant V_a, the coefficient of T_L is the Speed Regulation or rate of decrease of speed ω_m with increase in load torque T_L.

Quality of motor drive is enhance by:

a. Fast response speed measured by settling time $t_s = 4\tau$. Where τ is the system dominant time constant.

b. Speed regulation being as low as possible. Ideally zero.

Speed response is majorly determined by the roots of the characteristic equation:

$$s^2 + 2\varepsilon\omega_n s + \omega_n^2 = 0 \quad \textbf{(19)}$$

For second order system, s is evaluated as,

$$s = -\varepsilon\omega_n \pm \omega_n\sqrt{\varepsilon^2 - 1} \quad \textbf{(20)}$$

The real part of s being negative means that the system is stable; otherwise the system is unstable.

With second order system, the settling time t_s is approximated as 4τ. The response is:

$$f(t) = C_o + C_1 e^{(-\varepsilon\omega_n + \omega_n\sqrt{\varepsilon^2-1})t} + C_2 e^{(-\varepsilon\omega_n - \omega_n\sqrt{\varepsilon^2-1})t} \quad \textbf{(21)}$$

$$f(t) = C_o + C_1 e^{s_1 t} + C_2 e^{s_2 t} \quad \textbf{(22)}$$

Where, $f(t)$ can be the speed $\omega(t)$ or the current $i_a(t)$. If s_1 and s_2 are comparable in magnitude, both determine the response speed. If s_1 is ten or more times higher than s_2 or s_2 ten or more times higher in magnitude than s_1, the smaller root is the dominant root that determines the system speed response. In most dc motors, s_1 is much less in magnitude than s_2 and therefore determines the response. This makes the settling time $t_s = 4/s_1$

CLOSED LOOP SPEED CONTROL

Closed loop control improves on the drives performance by increasing speed of response and improving on speed regulation. So the functions of closed loop control is that ω_n is increased, ε is reduced, t_s is reduced, and Speed Regulation (SR) is reduced [6]. A closed loop speed control scheme is shown below.

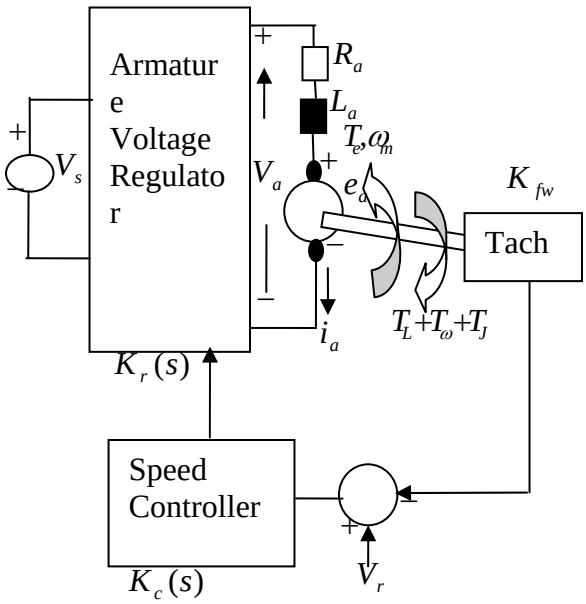

Figure 3: Schematic Diagram of the Closed Loop Speed Control.

Where,

$K_{f\omega}(s)$ is the tachometer feedback gain

$K_c(s)$ is the speed controller gain

$K_r(s)$ is the armature voltage regulator gain

Designating $K_c(s) * K_r(s) = K_{c\omega}(s)$, the block diagram representation of the control configuration is shown below.

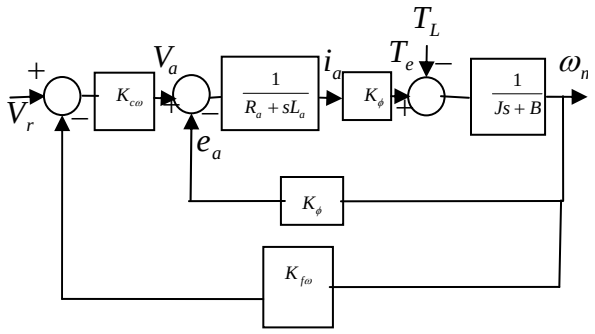

Figure 4: Block Diagram of the Closed Loop Speed Control.

The dynamic equation by mason's rule is,

$$\begin{pmatrix}\omega_m \\ i_a\end{pmatrix} = \frac{\begin{pmatrix} K_\phi K_{c\omega}(s) & -(R_a + sL_a) \\ (Js+B)K_{c\omega}(s) & K_\phi K_{f\omega}(s) K_{c\omega}(s)\end{pmatrix}\begin{pmatrix}V_r \\ T_L\end{pmatrix}}{D_o(s)} \quad \textbf{(23)}$$

Where,

$$D_o(s) = s^2 JL_a + (R_a J + BL_a)s + R_a B + K_\phi^2 + K_\phi K_{f\omega}(s) K_{c\omega}(s) \quad \textbf{(24)}$$

$$D_o(s) = JL_a[s^2 + (\frac{R_a J + BL_a}{JL_a})s + \frac{R_a B + K_\phi^2 + K_\phi K_{f\omega}(s) K_{c\omega}(s)}{JL_a} \quad \textbf{(25)}$$

If the tachometer loop does not contain a filter, the feedback gain can be a constant designated as $K_{f\omega}$.

$$K_{c\omega}(s) = K_{c\omega p} + \frac{K_{c\omega I}}{s} + sK_{cwd} \rightarrow PID \quad \textbf{(26)}$$

Where,

$K_{c\omega d}$ is the proportional gain component of $K_{c\omega}(s)$, $K_{c\omega I}$ is the integral gain component of $K_{c\omega}(s)$ and $K_{c\omega d}$ is the derivative gain component of $K_{c\omega}(s)$.

Three possible controller configurations are possible:

a. For $K_{c\omega I}$ and $K_{c\omega d}$ zero, $K_{c\omega}(s) = K_{c\omega p}$ which is a Proportional Controller (P-Controller).

b. For $K_{c\omega p}$ and $K_{c\omega d}$ zero, $K_{c\omega}(s) = \frac{K_{c\omega I}}{s}$ which is an Integral Controller (I-Controller).

c. For $K_{c\omega d}$ zero, $K_{c\omega}(s) = K_{c\omega p} + \frac{K_{c\omega I}}{s}$ which is a Proportional-Integral controller (PI-Controller).

Now taking the Proportional Controller as a case study, with $K_{c\omega}(s) = K_{c\omega p}$, the dynamic equation is,

$$\begin{pmatrix}\omega_m \\ i_a\end{pmatrix} = \frac{\begin{pmatrix} K_\phi K_{c\omega p} & -(R_a + sL_a) \\ (Js+B)K_{c\omega p} & K_\phi K_{f\omega} K_{c\omega p}\end{pmatrix}\begin{pmatrix}V_r \\ T_L\end{pmatrix}}{D_o(s)} \quad \textbf{(27)}$$

Where,

$$D_o(s) = s^2 JL_a + (R_a J + BL_a)s + R_a B + K_\phi^2 + K_\phi K_{f\omega} K_{c\omega p} \quad \textbf{(28)}$$

$$D_o(s) = JL_a[s^2 + (\frac{R_a J + BL_a}{JL_a})s + \frac{R_a B + K_\phi^2 + K_\phi K_{f\omega} K_{c\omega p}}{JL_a} \quad \textbf{(29)}$$

$$D_o(s) = JL_a[s^2 + 2\varepsilon\omega_n s + \omega_n^2] \quad \textbf{(30)}$$

Equation 30 is a second order system which when compared with Equation 29 results as follows:

The Natural Frequency of Oscillation, ω_n, is,

$$\omega_n = \sqrt{\frac{R_a B + K_\phi^2 + K_\phi K_{f\omega} K_{c\omega p}}{JL_a}} \qquad \textbf{(31)}$$

This is always higher than the open loop case due to the factor $K_\phi K_{f\omega} K_{c\omega p}$.

The Damping Ratio, ε, is

$$\varepsilon = \frac{R_a J + BL_a}{2\omega_n JL_a} \qquad \textbf{(32)}$$

This is lower than in the open loop case due to the increase in ω_n.

Speed Regulation (SR) is also derived as,

$$SR = \frac{-R_a}{R_a B + K_\phi^2 + K_\phi K_{f\omega} K_{c\omega p}} \qquad \textbf{(33)}$$

SR is also lower than in the open loop case due to the factor $K_\phi K_{f\omega} K_{c\omega p}$. This is an indication of a better drive performance.

INNER CURRENT LOOP CONTROL

Improvement in speed control can be obtained with Inner Current Loop Control method, whereby armature current is fed back to the input. A closed loop speed control scheme with inner current control is shown in Figure 5.

Designating $K_{ci}^{'} + K_r = K_{ci}$, the block diagram representation of the control configuration is shown in Figure 6.

The dynamic equation is,

$$\begin{pmatrix} \omega_m \\ i_a \end{pmatrix} = \frac{\begin{pmatrix} K_\phi K_{ci} K_{c\omega} & -(R_a + sL_a + K_{ci} K_{fi}) \\ (Js+B) K_{c\omega} K_{ci} & K_\phi + K_{f\omega} K_{c\omega} K_{ci} \end{pmatrix} \begin{pmatrix} V_r \\ T_L \end{pmatrix}}{D_o} \qquad \textbf{(34)}$$

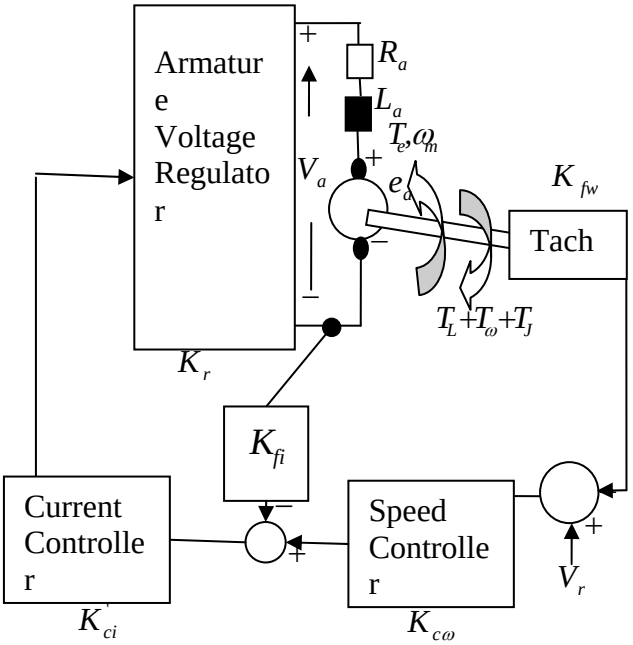

Figure 5: Schematic Diagram of the Inner Current Loop Control.

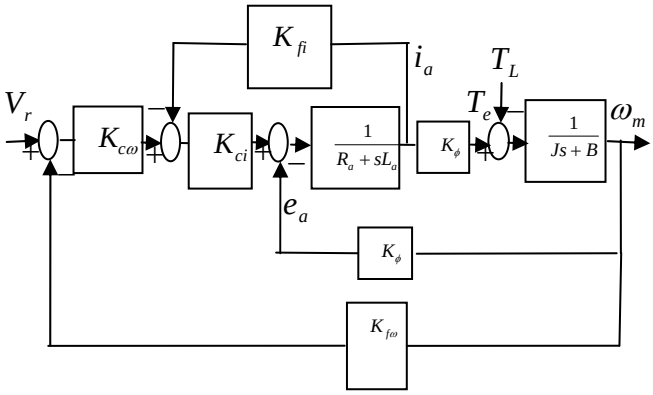

Figure 6: Block Diagram of the Inner Current Loop Control.

$$D_o = s^2 JL_a + (R_a J + BL_a + JK_{ci} K_{fi})s + R_a B + K_\phi^2 + K_{ci} K_{f\omega} K_{c\omega} + BK_{ci} K_{fi} \qquad \textbf{(35)}$$

MOTOR SIMULATIONS AND ANALYSIS

The Separately Excited DC Motor employed for analysis is rated 230V, 20A, 1500rpm and has the

Following parameters: $R_a = 1.0\Omega$, $L_a = 15mH$, $B = 0.01Nm\,\text{sec}/\,rad$, $K_\phi = 1.3369$, and $T_L = 26.738Nm$ (evaluated at steady).

These rated and evaluated parameters are employed in addition to the indicated values/configurations of controllers in Equations 10, 23, and 34 for the Open Loop Control, Closed Loop Speed Control , and the Inner Current Loop Control respectively for step changes in V_a, for the Open Loop Control and V_r for the Closed Loop Speed Control , and the Inner Current Loop Control. The models are simulated in SIMULINK® to yield the results as shown below.

OPEN LOOP CONTROL ANALYSIS

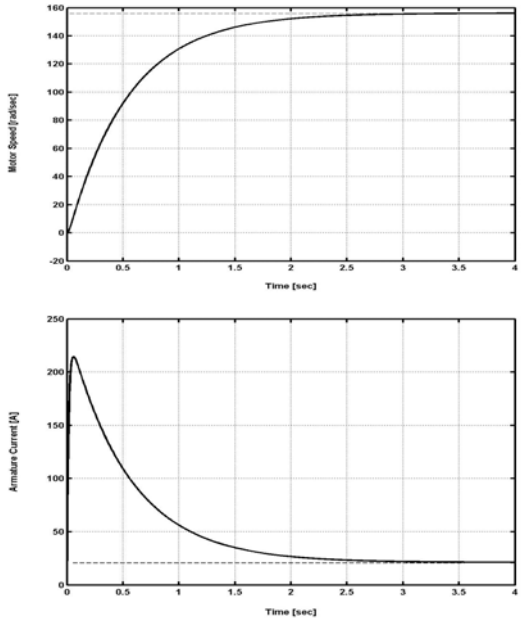

Figure 7: Motor Speed and Current Response for Open Loop Control.

CLOSED LOOP SPEED CONTROL

Proportional Controller (P-Controller)

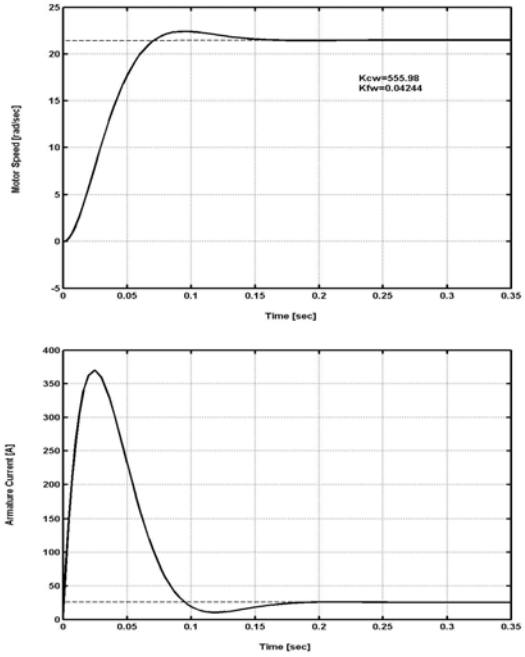

Figure 8: Motor Speed and Current Response with Proportional Speed Controller.

Integral Controller (I-Controller)

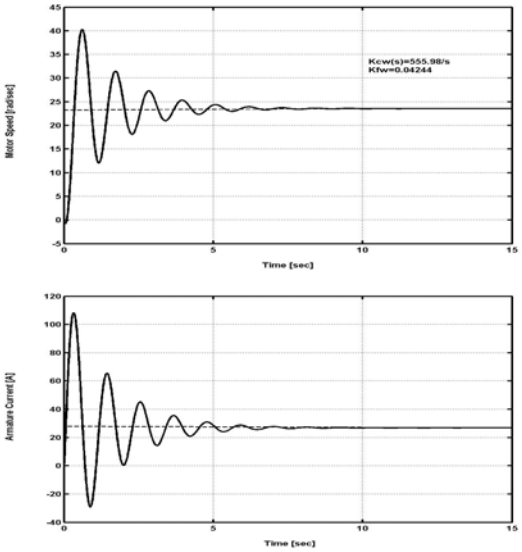

Figure 9: Motor Speed and Current Response with Integral Speed Controller.

Proportional-Integral Controller (PI-Controller)

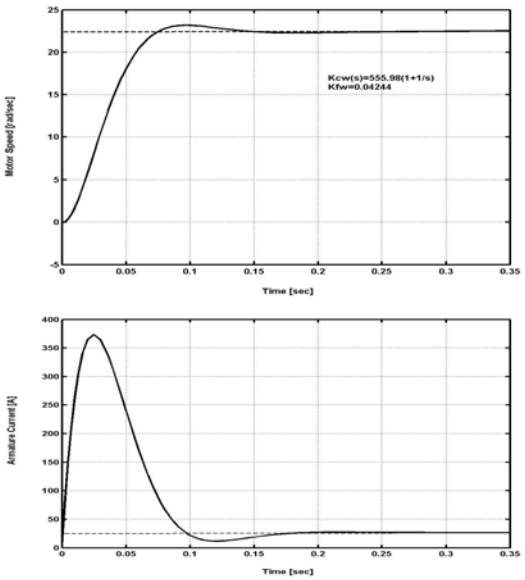

Figure 10: Motor Speed and Current Response with Proportional-Integral Speed Controller.

INNER CURRENT LOOP CONTROL

Proportional Controller (P-Controller)

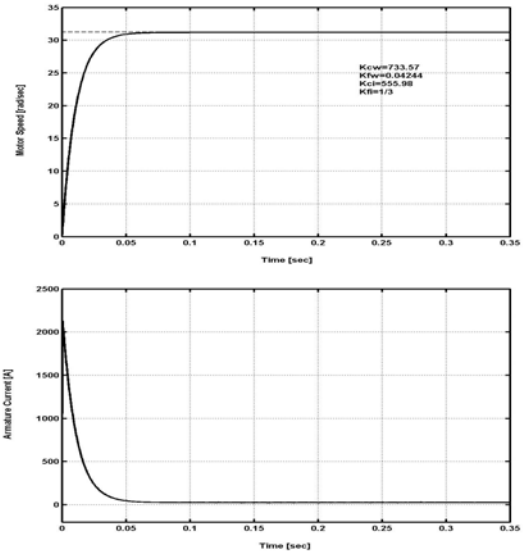

Figure 11: Motor Speed and Current Response with Inner Current Loop (P-Speed Controller).

Proportional-Integral Controller (PI-Controller)

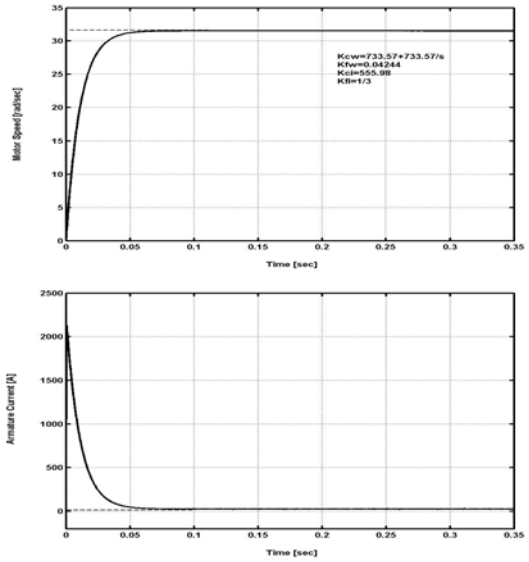

Figure 12: Motor Speed and Current Response with Inner Current Loop (PI- Speed Controller).

CONCLUSION

The step response of the Open Loop Control, as plotted in Figure 7, shows a sluggish response of speed and current with time. The dynamic state lasts longer before going into steady state than in other control methods as predicted by the dynamic equations. The Closed Loop Speed Control presents an enhanced control method with the Proportional and Proportional-Integral Controllers, in that order, as shown in Figure 8 and 10, respectively. The Integral Controller did not give a fast response as shown in Figure 9. The fastest response speed is obtained with the Inner Current Loop Control employing the Proportional and the Proportional-Integral Controllers, in that order, as shown in Figures 11 and 12, respectively. This method offers the best control benefits of increased speed response (reduced settling time) and improved (reduced) Speed Regulation.

REFERENCES

1. Okoro, O.I., C.U. Ogbuka, and M.U. Agu. 2008. “Simulation of D.C. Machines Transient Behaviors: Teaching and Research”. *Pacific Journal of Science and Technology*. 9(1):142-148.

2. Slemon, G.R. and Straughen, A. 1982. *Electric Machines*. Addison Wesley Publishing Company: New York, NY.

3. Moleykutty, G. 2008. ‘‘Speed Control of Separately Excited DC Motor’’. *American Journal of Applied Sciences*. 5(3): 227-233.

4. Ryff, D., Platnick, D., and Karnas, J. 1987. *Electric Machines and Transformers, Principles and Application*. Prentice-Hall Inc.: Englewood, NJ.

5. Wildi, T. 2000. *Electric Machines, Drives, Power Systems*. Prentice-Hall Inc.: Englewood, NJ.

6. Agu, M.U. 2007/2008 Session. ‘‘Electric Machine Drives’’. Unpublished Course Notes for EE 614, Department of Electrical Engineering, University of Nigeria, Nsukka.

ABOUT THE AUTHOR

Engr. Ogbuka, **Cosmas Uchenna** received his B.Eng. (First Class Honors) and M.Eng. degrees in 2004 and 2008, respectively, in the Department of Electrical Engineering University of Nigeria, Nsukka where he presently works as a Lecturer/Research Student. His research interests are in Adjustable Speed Drives of Electrical Machines: (DC and AC Electric Machine Torque/Speed Control with Converters and Inverters) and Power Electronics.

SUGGESTED CITATION

Ogbuka, C.U. 2009. “Performance Characteristics of Controlled Separately Excited DC Motor”. *Pacific Journal of Science and Technology*. 10(1):67-74.